

Deoxyribonucleoside Cyclic *N*-Acylphosphoramidites as a New Class of Monomers for the Stereocontrolled Synthesis of Oligothymidylyl- and Oligodeoxycytidylyl- Phosphorothioates

Andrzej Wilk, Andrzej Grajkowski, Lawrence R. Phillips,[†] and Serge L. Beaucage*

Contribution from the Division of Therapeutic Proteins, Center for Biologics Evaluation and Research, Food and Drug Administration, 8800 Rockville Pike, Bethesda, Maryland 20892, and Laboratory of Drug Discovery Research and Development, Developmental Therapeutics Program, National Cancer Institute, Frederick, Maryland 21701

Received May 28, 1999

Abstract: A simple and straightforward synthesis of the pyrimidine 2'-deoxyribonucleoside cyclic *N*-acylphosphoramidites **Rp-1** and **Sp-1** is described. Specifically, (±)-2-amino-1-phenylethanol **2** was chemoselectively *N*-acylated to **4** by treatment with ethyl fluoroacetate **3** followed by reaction with hexaethylphosphorus triamide to afford the cyclic *N*-acylphosphoramidite **5** as a mixture of diastereomeric rotamers (**5a** and **5b**). Condensation of *N*⁴-benzoyl-5'-*O*-(4,4'-dimethoxytrityl)-2'-deoxycytidine **8** with **5** in the presence of 1*H*-tetrazole gave, after silica gel chromatography, pure **Rp-1** and **Sp-1**. ³¹P NMR studies indicated that when **Rp-1** or **Sp-1** is reacted with 3'-*O*-acetylthymidine and *N,N,N',N'*-tetramethylguanidine in CD₃CN, the dinucleoside phosphotriester **Sp-9** or **Rp-9** is formed in near quantitative yield with total *P*-stereospecificity (δ_P 144.2 or 143.9 ppm, respectively). Sulfurization of **Sp-9** or **Rp-9** generated the *P*-stereodefined dinucleoside phosphorothioate **Rp-11** or **Sp-11** (δ_P 71.0 or 71.2 ppm, respectively). The 2'-deoxycytidine cyclic *N*-acylphosphoramidite derivatives **Rp-1** and **Sp-1** were subsequently applied to the solid-phase synthesis of [Rp,Rp]- and [Sp,Sp]-trideoxycytidyl diphosphorothioate d(C_{PS}C_{PS}C), and [Rp,Sp,Rp]-tetradexocytidyl triphosphorothioate d(C_{PS}C_{PS}C_{PS}C). Following deprotection, reversed-phase (RP) HPLC analysis of these oligonucleotide analogues showed a single peak for each oligomer. By comparison, RP-HPLC analysis of purified *P*-diastereomeric d(C_{PS}C_{PS}C) and d(C_{PS}C_{PS}C_{PS}C) prepared from standard 2-cyanoethyl deoxyribonucleoside phosphoramidites exhibited 4 and 8 peaks, respectively, each peak corresponding to a specific *P*-diastereomer (see Figure 3A). The thymidine cyclic *N*-acylphosphoramidite derivatives **Rp-14** and **Sp-14** were also prepared, purified, and used successfully in the solid-phase synthesis of [Rp]₁₁-d[(T_{PS})₁₁T]. Thus, the application of deoxyribonucleoside cyclic *N*-acyl phosphoramidites to *P*-stereocontrolled synthesis of oligodeoxyribonucleoside phosphorothioates may offer a compelling alternative to the methods currently used for such syntheses.

Oligodeoxyribonucleoside phosphorothioates (PS-ODNs) have been and continue to be extensively studied as potential therapeutic agents against various types of cancer and infectious diseases in humans.¹ Given that these oligonucleotide analogues are *P*-chiral, each of the *n* internucleotidic phosphorothioate linkages adopts either a *R_P* or a *S_P* configuration. Chemically synthesized PS-ODNs are therefore mixtures of 2ⁿ stereoisomers, the ratio *R_P*:*S_P* of these varying between 1:1 and 3:2.² Most studies addressing the biological activity, pharmacokinetic properties, and toxicology of PS-ODNs have been performed with oligonucleotides having undefined phosphorus chirality. Recently, stereopure *R_P*-oligodeoxyribonucleoside phosphorothioates were prepared enzymatically and then shown to possess a lower stability to nucleases endogenous to human serum than the parent PS-ODNs with undefined *P*-chirality.³ Conversely, chemically synthesized stereopure *S_P*-oligodeoxyribonucleoside

phosphorothioates have demonstrated superior stability to these nucleases than *P*-diastereomeric PS-ODNs.⁴ Thus, further investigation into the biological, pharmacokinetic, and toxicological properties of *P*-stereopure PS-ODNs requires improved chemical methods to synthesize these biomolecules and increase their availability for clinical studies.

Over the years, a number of methods have been developed for the preparation of PS-ODNs with defined *P*-chirality. Specifically, nucleoside oxathiaphospholane derivatives,⁵ cyclic phosphoramidites such as nucleoside indol-oxazaphosphorines⁶ or xylose-derived oxazaphosphorinanes,⁷ and nucleoside bicyclic

(3) Tang, J. Y.; Roskey, A.; Li, Y.; Agrawal, S. *Nucleosides Nucleotides* **1995**, *14*, 985–990.

(4) Koziolkiewicz, M.; Wojcik, M.; Kobylanska, A.; Karwowski, B.; Rebowska, B.; Guga, P.; Stec, W. J. *Antisense Nucleic Acid Drug Dev.* **1997**, *7*, 43–48.

(5) (a) Stec, W. J.; Grajkowski, A.; Koziolkiewicz, M.; Uznanski, B. *Nucleic Acids Res.* **1991**, *19*, 5883–5888. (b) Stec, W. J.; Grajkowski, A.; Kobylanska, A.; Karwowski, B.; Koziolkiewicz, M.; Misiura, K.; Okruszek, A.; Wilk, A.; Guga, P.; Boczkowska, M. *J. Am. Chem. Soc.* **1995**, *117*, 12019–12029. (c) Karwowski, B.; Guga, P.; Kobylanska, A.; Stec, W. J. *Nucleosides Nucleotides* **1998**, *17*, 1747–1759. (d) Stec, W. J.; Karwowski, B.; Boczkowska, M.; Guga, P.; Koziolkiewicz, M.; Sochacki, M.; Wiczorek, M. W.; Blaszczyk, J. *J. Am. Chem. Soc.* **1998**, *120*, 7156–7167.

(6) (a) Wang, J.-C.; Just, G. *Tetrahedron Lett.* **1997**, *38*, 3797–3800. (b) Wang, J.-C.; Just, G. *Tetrahedron Lett.* **1997**, *38*, 705–708.

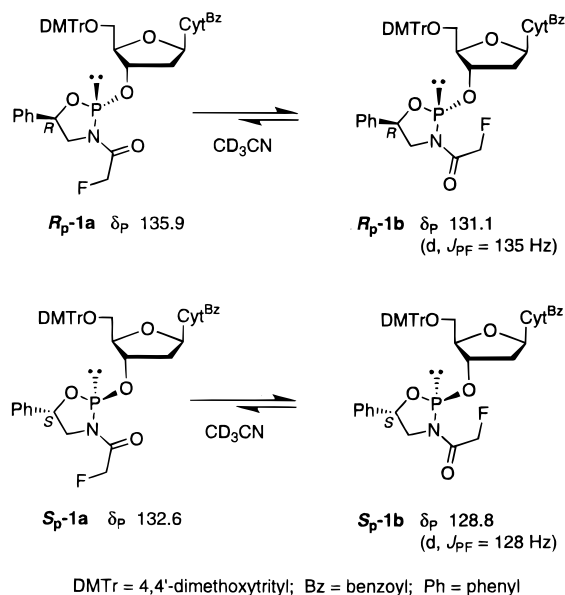
* To whom correspondence should be addressed. Telephone: (301)-827-5162. FAX: (301)-480-3256. E-mail: beaucage@phosphoramidite.cber.nih.gov.

[†] National Cancer Institute.

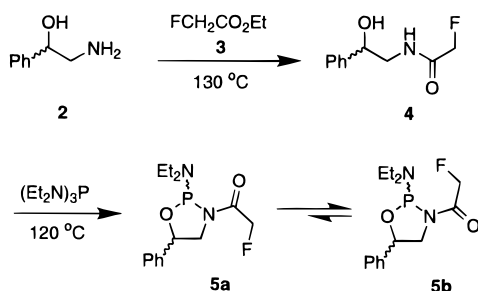
(1) (a) Croke, S. T.; Bennett, C. F. *Annu. Rev. Pharmacol. Toxicol.* **1996**, *36*, 107–129. (b) Beaucage, S. L.; Iyer, R. P. *Tetrahedron* **1993**, *49*, 6123–6194.

(2) (a) Wilk, A.; Stec, W. J. *Nucleic Acids Res.* **1995**, *23*, 530–534. (b) Wyrzykiewicz, T. K.; Cole, D. L. *Bioorg. Chem.* **1995**, *23*, 33–41.

Scheme 1



Scheme 2

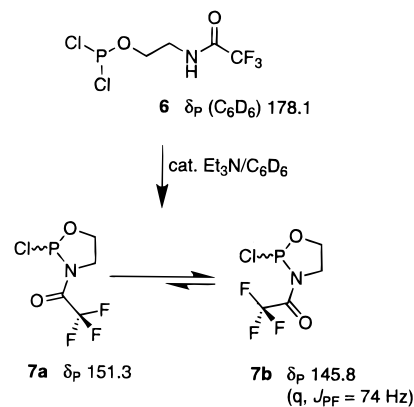


oxazaphospholidines⁸ have been used for this purpose. To date, only nucleoside oxathiaphospholane derivatives have enabled the synthesis of PS-ODNs with total *P*-stereospecificity. We now wish to report deoxyribonucleoside cyclic *N*-acylphosphoramidites, such as **R_P-1** and **S_P-1** (Scheme 1), as a promising new class of monomers in the *P*-stereospecific synthesis of PS-ODNs.

Results and Discussion

The synthesis of **R_P-1** and **S_P-1** begins with the preparation of cyclic *N*-acylphosphoramidite **5** (Scheme 2). Commercial (±)-2-amino-1-phenylethanol **2** was reacted with ethyl fluoroacetate **3** (1.3 equiv) at 130 °C until ethanol had completely distilled off to afford the crude amido alcohol **4** in near quantitative yields. Heating recrystallized **4** with hexaethylphosphorus triamide (1 equiv) at 120 °C until *N,N*-diethylamine had distilled off⁹ was followed by distillation of the material left under high-vacuum to give **5** as a viscous liquid. The cyclic *N*-acylphosphoramidite **5** was characterized by NMR spectroscopy and accurate mass determination. ¹H and ¹³C NMR spectra of **5** are quite complex due to the presence of rotamers **5a** and

Scheme 3



5b as a consequence of partial double-bond character of the C–N bond linking the 2-fluoroacetyl group to the oxazaphospholane ring.¹⁰ Further, we found the ratio of these rotamers to vary with solvent polarity.¹¹ Other factors contributing to the complexity of NMR data are ¹H and ¹³C spin–spin couplings to phosphorus and fluorine. In this regard, the proton-decoupled ³¹P NMR spectrum of **5** in C₆D₆ or DMSO-*d*₆ is simpler to analyze.

Because **5** possesses two chiral centers, two sets of two signals at ~120 and ~130 ppm are observed due to the tricoordinated phosphorus atom (**R_P** and **S_P**). Each set of signals (**R_P** or **S_P**) can be assigned to the two rotamers, one of which appears as a singlet (**5a**) and the other (**5b**) as a doublet. Given the large coupling constants ($J_{PF} = 50\text{--}75$ Hz) associated with the signal observed for **5b** in solvents of differing polarity, it is likely that these signals result from “through-space” ³¹P–¹⁹F spin–spin coupling.¹² Additional evidence in support of these spectral assessments was obtained from an experiment involving base-induced cyclization of 2-[*N*-(2,2,2-trifluoroacetyl)amino]ethyl phosphordichloridite **6** to the chloro *N*-acylphosphoramidite derivative **7** as a mixture of rotamers (**7a** and **7b**) in CD₃CN (Scheme 3). Proton-decoupled ³¹P NMR analysis of this mixture showed signals at 178 ppm (singlet assigned to the dichloridite **6**), 151 ppm (singlet corresponding to rotamer **7a**), and 146 ppm (quartet attributed to rotamer **7b** which has its fluorine atoms crowded near the phosphorus atom).¹³ The quartet (characterized by a ³¹P–¹⁹F spin–spin coupling constant $J_{PF} = 74$ Hz) indicates through-space or nonbonded interactions between the phosphorus and fluorine nuclei. To the best of our knowledge, a “through-bond” ⁴ J_{PF} would be expected to be less than 5 Hz.¹⁴ Our observations are consistent with those reported in the

(10) Multiplicity of ¹H, and ¹³C NMR signals associated with tertiary amide rotamers is well-documented in the literature; for example, see: (a) Abraham, R. J.; Loftus, P. In *Proton and Carbon-13 NMR Spectroscopy - An Integrated Approach*; Heyden: London, 1980; pp 171–174. (b) Edwards, O. E.; Dvornik, D.; Kolt, R. J.; Blackwell, B. A. *Can. J. Chem.* **1992**, *70*, 1397–1405. (c) Hoye, T. R.; Renner, M. K. *J. Org. Chem.* **1996**, *61*, 2056–2064. (d) Wilk, A.; Grajkowski, A.; Phillips, L. R.; Beaucage, S. L. *J. Org. Chem.* **1999**, *64*, 7515–7522.

(11) A striking example of chemical shift dependence upon solvent polarity is illustrated by the ³¹P NMR spectra of **5** in C₆D₆ and DMSO-*d*₆ (data shown as Supporting Information). The signal intensity of rotameric species **5a** in C₆D₆ (123.5 and 133.1 ppm) is reduced by at least a factor of 5 in DMSO-*d*₆.

(12) Proton-coupled ¹⁹F NMR analysis of **5** exhibited two sets (one for **R_P** and the other for **S_P**) of two signals. Each set of signals was composed of a triplet attributed to rotamer **5a** and two triplets assigned to rotamer **5b**. The signals associated with **5b** (12 lines for overlapping **R_P-5b** and **S_P-5b**) resulted from ³¹P–¹⁹F spin–spin coupling; the coupling constants J_{PF} (53 and 70 Hz in C₆D₆) were identical to the J_{PF} measured from the corresponding ³¹P NMR spectrum (data shown in Experimental section and as Supporting Information).

(13) Data shown as Supporting Information.

(7) (a) Jin, Y.; Just, G. *J. Org. Chem.* **1998**, *63*, 3647–3654. (b) Jin, Y.; Biancotto, G.; Just, G. *Tetrahedron Lett.* **1996**, *37*, 973–976.

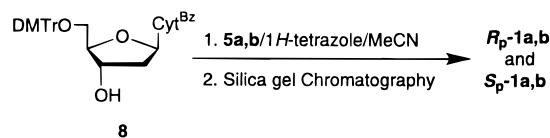
(8) (a) Iyer, R. P.; Guo, M.-J.; Yu, D.; Agrawal, S. *Tetrahedron Lett.* **1998**, *39*, 2491–2494. (b) Guo, M.-J.; Yu, D.; Iyer, R. P.; Agrawal, S. *Bioorg. Med. Chem. Lett.* **1998**, *8*, 2539–2544 and references therein.

(9) This reaction was carried out essentially as described in the literature; see: (a) Mizrakh, L. I.; Polonskaya, L. Yu.; Kozlova, L. N.; Babushkina, T. A.; Bryantsev, B. I. *Zh. Obshch. Khim.* **1975**, *45*, 1469–1473. (b) Pudovik, M. A.; Terent'eva, S. A.; Medvedeva, M. D.; Pudovik, A. N. *Zh. Obshch. Khim.* **1973**, *43*, 679.

literature; through-space ^{31}P – ^{19}F spin–spin couplings were found for (*o*-trifluoromethylphenyl) phosphines with J_{PF} values ranging from 51 to 56 Hz in chlorobenzene.¹⁵ Finally, through-space ^{19}F – ^{19}F spin–spin couplings have been extensively studied¹⁶ in 1,8-difluoronaphthalene and 4,5-difluorophenanthrene derivatives. In these compounds, the intramolecular pairs of fluorine atoms crowded near each other exhibited large coupling constants ($J_{\text{FF}} = 59$ – 177 Hz).^{17–19}

Condensation of commercial *N*⁴-benzoyl-5'-*O*-(4,4'-dimethoxytrityl)-2'-deoxycytidine **8** with **5** (1.1 equiv) and 1*H*-tetrazole (1.1 equiv) was carried out in dry acetonitrile for 20 min at 25 °C. The crude reaction products were purified by chromatography on silica gel 60 (230–400 mesh) to afford **R_p-1** and **S_p-1**²⁰ as white amorphous solids.²¹ Although pure (>99%), the relatively low yield of these cyclic *N*-acylphosphoramidites (26 and 22%, respectively) is due to only modest stability of **R_p-1** and **S_p-1** toward silica gel chromatography. The stability of deoxyribonucleoside cyclic *N*-acylphosphoramidites during chromatography depends, in part, on the nature of the *N*-acyl and C-5 functional groups of the oxazaphospholane ring.²² Typically, the stability of deoxyribonucleoside cyclic *N*-acylphosphoramidites toward silica gel decreases in the following order: *N*-propionyl > *N*-acetyl > *N*-(2-methoxyacetyl) > *N*-(2-fluoroacetyl) ≫ *N*-(2,2,2-trifluoroacetyl). Stability also decreases with the following substitution in the C-5 group of the oxazaphospholane ring: phenyl > allyl > H. The most critical feature in the purification of **R_p-1** and **S_p-1** by silica gel chromatography is minimizing the contact time of these cyclic *N*-acylphosphoramidites with silica gel. However, this must be performed in a manner that would not compromise the chromatographic resolution of these *P*-stereopure phosphor-

amidite derivatives.²³ Thus, column dimensions, amount of sorbent, elution solvent(s), and flow rates must be optimized to ensure the best chromatographic resolution of *P*-stereodefined phosphoramidite derivatives within the shortest period of time. Although the silica gel-induced decomposition products of **R_p-1** and **S_p-1** have not yet been completely characterized, small amounts (less than 5%) of hydrolyzed **S_p-1** (presumably its *H*-phosphonate derivative) and deoxyribonucleoside **8** can be generated during chromatography. A fraction of these decomposition products co-elute with the slower-moving **R_p-1**. When purified and isolated as amorphous solids, cyclic *N*-acylphosphoramidites **R_p-1** and **S_p-1** exhibit stability comparable to that of the parent 2-cyanoethyl 2'-deoxycytidine phosphoramidite in either long-term storage or in acetonitrile solution. Selection criteria for the oxazaphospholane *N*-(2-fluoroacetyl) and C-5 phenyl groups of deoxyribonucleoside cyclic *N*-acylphosphoramidites were thus based on the excellent solid-state and solution stability of **R_p-1** and **S_p-1**, their coupling efficiency in solid-phase oligonucleotide synthesis, and the relative ease of oligonucleotidic phosphate/phosphorothioate triester deprotection.



The 2'-deoxycytidine cyclic *N*-acylphosphoramidites **R_p-1** and **S_p-1** were characterized by NMR spectroscopy, accurate mass determination, and HPLC. Much like the ^1H and ^{13}C NMR spectra of **5**, those of **R_p-1** and **S_p-1** are difficult to interpret due to the presence of rotamers (**R_p-1a** and **R_p-1b**, **S_p-1a** and **S_p-1b**) and $^1\text{H}/^{13}\text{C}$ spin–spin couplings to phosphorus and fluorine. As demonstrated in the case of **5**, proton-decoupled ^{31}P NMR spectra of **R_p-1** and **S_p-1** are more amenable to interpretation. Typically, a signal (doublet) is observed at ~ 130 ppm in CD_3CN and assigned to the rotamer **R_p-1b** or **S_p-1b** that has the fluorine and phosphorus atoms near to each other (Scheme 1 and Figure 1).²⁴ This doublet originates from a through-space ^{31}P – ^{19}F spin–spin coupling and is characterized by a large coupling constant ($J_{\text{PF}} \sim 131$ Hz). Additionally, a singlet is present at ~ 134 ppm and attributed to the rotamer **R_p-1a** or **S_p-1a** that has the fluorine and the phosphorus atoms distal to each other; no ^{31}P – ^{19}F spin–spin coupling could be measured for that rotamer. A proton-coupled ^{19}F NMR spectrum of **S_p-1** revealed two signals at -224 ppm and -219 ppm in C_6D_6 relative to fluorotrichloromethane that was used as an external standard.¹³ The signal at -224 ppm (set of two triplets) is tentatively assigned to the rotamer **S_p-1a** given the small ^{19}F – ^{31}P spin–spin coupling constant $^4J_{\text{FP}} = 2.1$ Hz measured for that rotamer. The signal observed at -219 ppm (set of two triplets) is attributed to the rotamer **S_p-1b**, as it probably resulted from a through-space ^{19}F – ^{31}P spin–spin coupling; a large coupling constant ($J_{\text{FP}} = 181$ Hz) was measured for that signal.

(23) Complete elution of deoxyribonucleoside cyclic *N*-acylphosphoramidites from silica gel columns should be accomplished within 2 h to minimize decomposition.

(24) Both **R_p-1** and **S_p-1** used for the reactions performed in NMR tubes (Figure 1) have been scrupulously purified. Specifically, **R_p-1** has been purified twice to prevent its contamination with small amounts of **8** generated by the slow decomposition of **S_p-1** during silica gel chromatography. The presence of **8** during the activation of **R_p-1** with TMG would lead to the formation of the corresponding (3'-3')-dinucleoside phosphite triester. Given the similarity of the ^{31}P NMR chemical shift of this phosphite triester with that of **R_p-9** and **S_p-9**, its presence may incorrectly be viewed as an apparent lack of coupling stereospecificity during the preparation of **S_p-9**.

(14) Hund, R.-D.; Behrens, U.; Röschenhaler, G.-V. *Phosphorus, Sulfur, Silicon* **1992**, *69*, 119–127.

(15) Miller, G. R.; Yankowsky, A. W.; Grim, S. O. *J. Chem. Phys.* **1969**, *51*, 3185–3190.

(16) (a) Everett, T. S. In *Chemistry of Organic Fluorine Compounds II - A Critical Review*, ACS Monograph 187; Hudlický, M., Pavlath, A. E., Eds.; American Chemical Society: Washington, DC, 1995; pp 1037–1086.

(b) Servis, K. L.; Fang, K.-N. *J. Am. Chem. Soc.* **1968**, *90*, 6712–6717. (c) Chambers, R. D.; Sutcliffe, L. H.; Tiddy, G. J. T. *Trans. Faraday Soc.* **1970**, *66*, 1025–1038. (d) Hilton, J.; Sutcliffe, L. H. *Prog. Nucl. Magn. Reson. Spectros.* **1975**, *10*, 27–39. (e) Matthews, R. S.; Preston, W. E. *Org. Magn. Reson.* **1980**, *14*, 258–263. (f) Matthews, R. S. *Org. Magn. Reson.* **1982**, *18*, 226–230.

(17) Mallory, F. B.; Mallory, C. W.; Fedarko, M.-C. *J. Am. Chem. Soc.* **1974**, *96*, 3536–3542.

(18) Mallory, F. B.; Mallory, C. W.; Ricker, W. M. *J. Am. Chem. Soc.* **1975**, *97*, 4770–4771.

(19) Mallory, F. B.; Mallory, C. W.; Ricker, W. M. *J. Org. Chem.* **1985**, *50*, 457–461.

(20) The *P*-stereochemistry of these deoxyribonucleoside cyclic *N*-acylphosphoramidites has been tentatively assigned on the basis that the relative RP-HPLC mobility of [**R_p**,**S_p**,**R_p**]-d(**C_{ps}C_{ps}C_{ps}C**) prepared from **R_p-1** and **S_p-1** corresponded to that reported for a d(**C_{ps}C_{ps}C_{ps}C**) diastereomer of identical *P*-stereochemistry that was assigned according to known procedures (see ref 2a). Assuming that base-assisted coupling of the 5'-OH function of nucleosides and nucleotides with **R_p-1** or **S_p-1** occurred with inversion of configuration at phosphorus, and sulfurization of the resulting phosphite triester proceeded with retention of configuration, our tentative *P*-stereochemical assignments for **R_p-1** and **S_p-1** seem justified. NMR experiments are currently underway to confirm the absolute *P*-stereochemistry of **R_p-1** and **S_p-1**. In addition, the stereochemistry of these *N*-acylphosphoramidites at C-5 of the oxazaphospholane ring has been determined by an alternate synthesis of **R_p-1** and **S_p-1** using enantiomerically pure 2-amino-1-phenylethanol, and comparing chromatographic and ^{31}P NMR properties. It is still unclear why only **R_p-1** and **S_p-1**, out of potentially four diastereomers, can be isolated.

(21) HPTLC–RP2F (Analtech): **R_p-1**, R_f (CHCl_3 : CH_3CN 2:1 v/v) = 0.51; **S_p-1**, R_f (CHCl_3 : CH_3CN 2:1 v/v) = 0.71.

(22) Numbering nomenclature of the oxygen, phosphorus, and nitrogen atoms of the oxazaphospholane ring is 1, 2, and 3, respectively. See: *Phosphor-Verbindungen II, Houben-Weyl - Methoden der organischen Chemie, Band E2*; Georg Thieme Verlag Stuttgart: New York, 1982; pp 1125–1126.

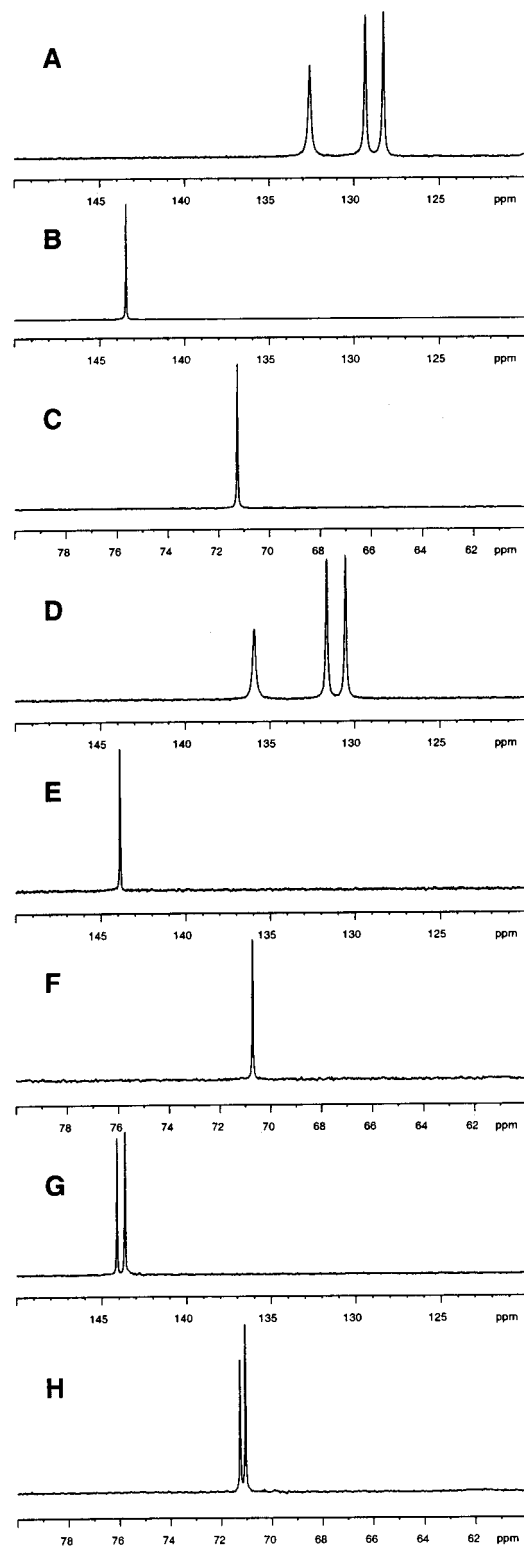
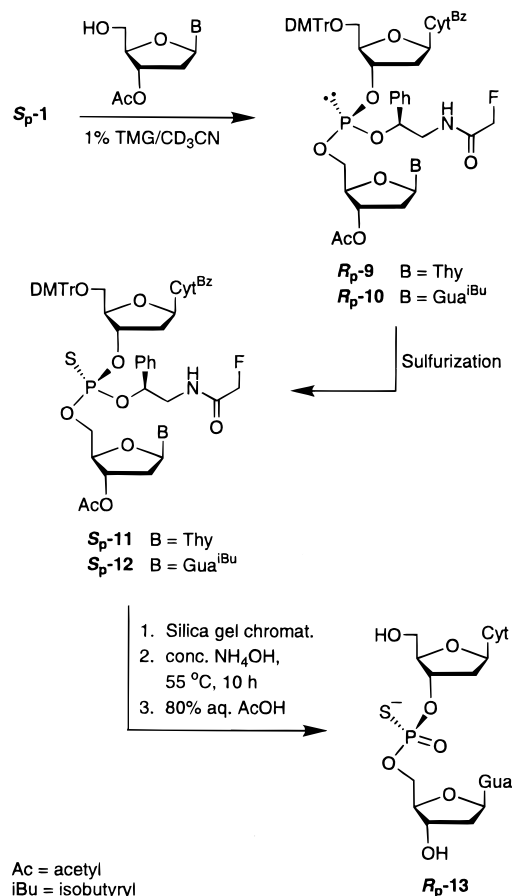


Figure 1. ^{31}P NMR (121 MHz, CD_3CN) spectra of: (A) $S_{\text{P}}\text{-1}$ as a mixture of rotamers $S_{\text{P}}\text{-1a}$ and $S_{\text{P}}\text{-1b}$; (B) $R_{\text{P}}\text{-9}$ generated from $S_{\text{P}}\text{-1}$ and 3'-*O*-acetylthymidine in the presence of TMG; (C) $S_{\text{P}}\text{-11}$ obtained by sulfurization of $R_{\text{P}}\text{-9}$ with 3*H*-1,2-benzodithiol-3-one 1,1-dioxide; (D) $R_{\text{P}}\text{-1}$ as a mixture of rotamers $R_{\text{P}}\text{-1a}$ and $R_{\text{P}}\text{-1b}$; (E) $S_{\text{P}}\text{-9}$ generated from $R_{\text{P}}\text{-1}$ and 3'-*O*-acetylthymidine in the presence of TMG; (F) $R_{\text{P}}\text{-11}$ obtained by sulfurization of $S_{\text{P}}\text{-9}$ with 3*H*-1,2-benzodithiol-3-one 1,1-dioxide; (G) $R_{\text{P}}\text{-9}$ from (B) and $S_{\text{P}}\text{-9}$ from (E) mixed together; (H) $S_{\text{P}}\text{-11}$ from (C) and $R_{\text{P}}\text{-11}$ from (F) mixed together.

By comparison, the ^{31}P NMR signal assigned to $S_{\text{P}}\text{-1b}$ in C_6D_6 is a doublet at 126 ppm with a $J_{\text{PF}} = 182$ Hz. Because of ^{31}P NMR signal broadening, no through-bond ^{31}P – ^{19}F spin–spin

Scheme 4



coupling was observed for the signal corresponding to rotamer $S_{\text{P}}\text{-1a}$ at 133.0 ppm.¹³ Thus, the equivalence of J_{FP} and J_{PF} proves that the ^{31}P and ^{19}F NMR signals observed for $S_{\text{P}}\text{-1b}$ in C_6D_6 at 126 ppm and -219 ppm, respectively, result from a ^{31}P – ^{19}F spin–spin coupling. Although the absolute magnitude of J_{FP} and J_{PF} for $R_{\text{P}}\text{-1b}$ and $S_{\text{P}}\text{-1b}$ is larger in C_6D_6 than in CD_3CN , the relative magnitudes of J_{FP} and J_{PF} are identical for either $R_{\text{P}}\text{-1b}$ or $S_{\text{P}}\text{-1b}$ whether measured in C_6D_6 , CD_3CN , or a mixture of these solvents (data not shown).

Unlike standard deoxyribonucleoside phosphoramidites, $R_{\text{P}}\text{-1}$ and $S_{\text{P}}\text{-1}$ are not activated by weak acids; however, similar to deoxyribonucleoside oxathiaphospholane derivatives,⁵ they readily react with base-activated nucleophiles. For example, when $S_{\text{P}}\text{-1}$ is mixed with 3'-*O*-acetylthymidine (1.1 equiv) in CD_3CN in a NMR tube, addition of *N,N,N',N'*-tetramethylguanidine (TMG, 1% v/v) leads to rapid (<5 min) formation of the dinucleoside phosphite triester $R_{\text{P}}\text{-9}$ (Scheme 4 and Figure 1) in essentially quantitative yields with total *P*-stereospecificity. The ^{31}P NMR spectrum of $R_{\text{P}}\text{-9}$ showed only a single line (143.9 ppm), indicative of *P*-stereopurity. Sulfurization of $R_{\text{P}}\text{-9}$ with 3*H*-1,2-benzodithiol-3-one 1,1-dioxide^{25,26} afforded the *P*-stereodefined dinucleoside phosphorothioate triester $S_{\text{P}}\text{-11}$ ($\delta_{\text{P}} 71.2$ ppm) with complete stereospecificity (Figure 1).²⁶ Substituting *N*²-iso-

(25) (a) Beaucage, S. L.; Iyer, R. P.; Egan, W.; Regan, J. B. *Ann. New York Acad. Sci.* **1990**, *616*, 483–485. (b) Iyer, R. P.; Phillips, L. R.; Egan, W.; Regan, J. B.; Beaucage, S. L. *J. Org. Chem.* **1990**, *55*, 4693–4699. (c) Regan, J. B.; Phillips, L. R.; Beaucage, S. L. *Org. Prep. Proced. Int.* **1992**, *24*, 488–492.

(26) 3*H*-1,2-Benzodithiol-3-one 1,1-dioxide is unstable in the presence of TMG in the NMR tube. Consequently, more than the normally required amount of sulfur-transfer reagent is necessary for complete sulfurization. Due to extensive base-catalyzed decomposition of the sulfurizing reagent, variable amounts of oxidized, instead of sulfurized, dinucleoside phosphotriester is detected by ^{31}P NMR spectroscopy.

butyryl-3'-*O*-acetyl-2'-deoxyguanosine for 3'-*O*-acetylthymidine in Scheme 4 cleanly produced the *P*-stereodefined dinucleoside phosphite triester **R_p-10** (δ_P 143.9 ppm). After sulfurization, the corresponding dinucleoside phosphorothioate triester **S_p-12** (δ_P 71.2 ppm) was obtained.¹³ Under these conditions, *O*⁶-phosphitylation or other modification of the guanine nucleobase could not be detected. The dinucleotide analogue **S_p-12** was separated from excess *N*²-isobutyryl-3'-*O*-acetyl-2'-deoxyguanosine by silica gel chromatography prior to being treated with concentrated NH₄OH for 10 h at 55 °C. Following detritylation, RP-HPLC analysis of the deprotected dimer **R_p-13** revealed that two major products had been formed. One corresponded to **R_p-13** (single peak with t_R = 12.6 min, >95%), whereas the other (single peak with t_R = 16.4 min) was identified as benzamide.¹³ This side-product was produced by ammonolysis of *N*²-benzoylcytosine during deprotection. The identity of **R_p-13** was further confirmed, after deprotection, by comigration with one of the two RP-HPLC peaks associated with *P*-diastereomeric d(C_{PS}G) that was prepared from commercial 2-cyanoethyl phosphoramidites (data not shown).

Given that solid-phase coupling reactions usually occur with substantially slower kinetics than those performed in solution, both **R_p-1** and **S_p-1** were separately condensed with commercial *N*-protected 2'-deoxyguanosine linked to long-chain alkylamine controlled pore glass (LCAA-CPG). The condensation reaction required a higher concentration of TMG (5%, v/v) in acetonitrile to achieve coupling rates comparable to those obtained in solution phase. Following sulfurization, the solid-phase-linked dimer was acidified, and the coupling efficiency of **R_p-1** and **S_p-1** was estimated on the basis of the spectrophotometric measurement of the 4,4'-dimethoxytrityl cation absorbance at 498 nm. A coupling efficiency of ~98% was thus determined. Each *P*-stereopure dinucleoside phosphorothioate was released from the support and fully deprotected by treatment with concentrated NH₄OH for 10 h at 55 °C. The RP-HPLC profiles of **R_p-13** and **S_p-13** are, as expected, very similar to those obtained from solution-phase synthesis of **R_p-13** and **S_p-13**.¹³ Both **R_p-13** and **S_p-13** show as a single homogeneous peak (t_R = 12.6 and 13.4 min, respectively) indicative of high *P*-stereopurity. Benzamide appeared as a single peak (t_R = 16.4 min) and a small amount (<5%) of 2'-deoxyguanosine (t_R = 9.6 min) was detected in accordance with the results of the trityl assay performed prior to alkaline deprotection. The identities of minor RP-HPLC peaks (t_R = 10.6 min, <3%, t_R ≈ 12, 17.8, and 21.5 min, each representing less than 1% of the total peak area) are still unknown. However, these results show that formation of side-products during the solid-phase preparation of either **R_p-13** or **S_p-13** is minimal.¹³

Cleavage of the amidated benzyl thiophosphate-protecting group from **S_p-11** (**R_p-11**) or **S_p-12** (**R_p-12**) by concentrated NH₄OH is essentially complete within 10 h at 55 °C and is likely to proceed by more than one mechanism. For example, cyclo-deesterification of the amidated benzyl thiophosphate protecting group may follow path a (Figure 2) with the simultaneous formation of an oxazoline derivative. It has been reported that heating a 2-acetamidoethyl phosphite triester at 140–145 °C under vacuum leads to formation of 2-methyl-2-oxazoline.²⁷ It could therefore be argued that a cyclo-deesterification reaction could also occur when the leaving group is a thiophosphate instead of an *H*-phosphonate diester derivative. Indeed, when *N*- and 5'-*O*-deblocked **R_p**- or **S_p-12**²⁸ (Figure 2) was heated in the absence of NH₄OH in acetonitrile:H₂O (1:1

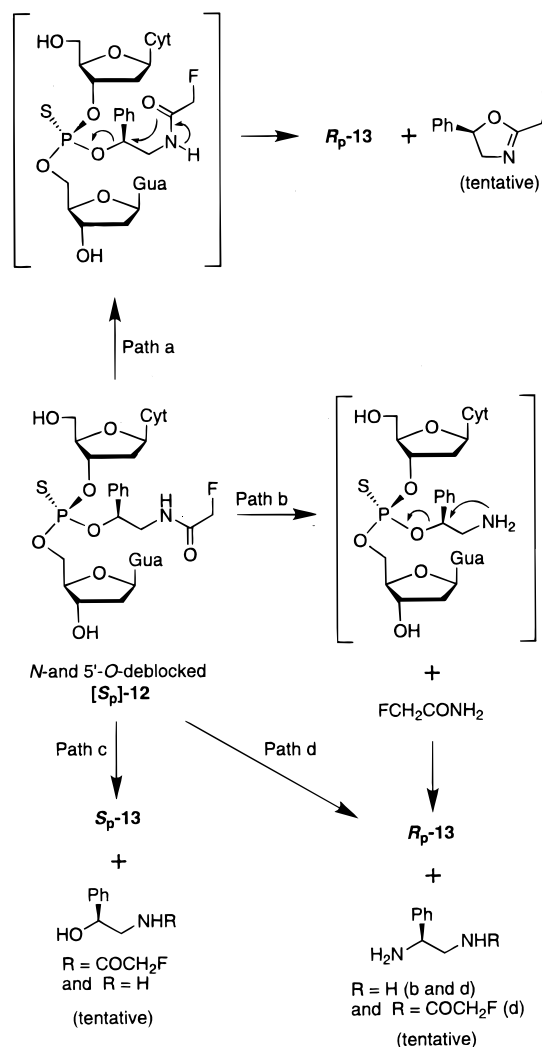


Figure 2. Possible pathways for the deprotection of internucleotidic phosphorothioate triester by treatment with concentrated NH₄OH at 55 °C using *N*- and 5'-*O*-deblocked **R_p-12** or **S_p-12** as a model. Path a: thermolytic cyclo-deesterification; path b: ammonolysis of the 2-fluoroacetyl group followed by cyclo-deesterification; path c: *P*-deesterification via S_N2 attack of ammonia and/or hydroxide at phosphorus; path d: *P*-deesterification via S_N2 attack of ammonia at the benzylic carbon.

v/v) for 1 h at 85 °C, **R_p-13** or **S_p-13** was produced in yields similar to those obtained under ammonolysis conditions (in accordance with the results of RP-HPLC analysis of the deprotection reaction).¹³ Under the reaction conditions used, path a is a viable mechanism for thiophosphate deprotection of **S_p-11** (**R_p-11**) or **S_p-12** (**R_p-12**).

Alternatively, ammonolysis of the 2-fluoroacetamido group could be envisioned to generate an aminoalkylated thiophosphate triester intermediate via path b (Figure 2), which could then readily induce cyclo-deesterification with concomitant formation of a highly reactive aziridine intermediate.²⁹ Cyclo-deesterification of aminoalkylated phosphotriesters is well-documented

(27) Mizrahi, L. I.; Polonskaya, L. Yu.; Babushkina, T. A.; Bryantsev, B. I. *Zh. Obshch. Khim.* **1975**, *45*, 549–552.

(28) Typically, *N*- and 5'-*O*-deblocked **S_p-12** was prepared by condensing **S_p-1** with dG^{bu}-LCAA-CPG in the presence of TMG in acetonitrile as recommended in the Experimental Section. Following sulfurization and detritylation, the solid-phase-linked dimer was exposed to pressurized ammonia gas (~10 bar) for 10 h at 25 °C (see ref 37). Under these conditions, the dimer is released from the support and *N*-deprotected without significant loss (<10%) of the amidated benzyl thiophosphate-protecting group. Ammonia free *N*- and 5'-*O*-deblocked **S_p-12** was then eluted from CPG using MeCN–H₂O (1:1 v/v) for further experimentation.

(29) Brown, D. M.; Osborne, G. O. *J. Chem. Soc.* **1957**, 2590–2593.

in the literature.^{10d,29,30} In agreement with predictions, we found that incubation of the fluoroacetamido alcohol **4** with concentrated NH_4OH at 55 °C for 10 h leads to substantial ammonolysis of the 2-fluoroacetamido group (~25%) as revealed by RP-HPLC analysis of the reaction. These findings strongly support path b as a concurrent cleavage mechanism of the amidated benzyl thiophosphate-protecting group from **Sp-11** (**Rp-11**) or **Sp-12** (**Rp-12**) by concentrated NH_4OH .

Another possibility is an $\text{S}_{\text{N}}2$ -type nucleophilic attack at phosphorus by ammonia and/or hydroxide ion that could lead to displacement of the amidated benzyl thiophosphate-protecting group with inversion of configuration at phosphorus (path c, Figure 2).³¹ This nucleophilic attack at phosphorus would also produce internucleotide bond cleavage with the generation of either 2'-deoxycytidine or 2'-deoxyguanosine along with their corresponding amidated or aminoalkylated phosphorothioate diesters.³¹ Although this pathway cannot be ruled out, our results do not support it as being an operative mechanism in *P*-deprotection of **Sp-11** (**Rp-11**) or **Sp-12** (**Rp-12**).

Finally, an $\text{S}_{\text{N}}2$ attack by ammonia at the benzylic carbon atom could displace the internucleotide thiophosphate function (path d, Figure 2). It is well-known that deprotection of benzyl phosphate and benzyl phosphorodithioate derivatives can be readily achieved by treatment with thiophenolates,³² presumably via $\text{S}_{\text{N}}2$ attack by the thiolate at the benzylic carbon atom. Although ammonia is a harder base than thiolates,³³ it has been reported to stereospecifically demethylate a dinucleoside methyl phosphorothioate triester to the corresponding phosphorothioate diester.³⁴ It is therefore conceivable that concentrated NH_4OH could cleave a benzylic thiophosphate protecting group under the conditions used for removing the methyl thiophosphate-protecting group.

Deprotection of the amidated benzyl thiophosphate-protecting group from **Sp-11** (**Rp-11**) or **Sp-12** (**Rp-12**) under basic conditions is indeed complex considering the many pathways that could lead to the formation of **Sp-13** or **Rp-13**. However, deprotection mechanisms according to paths a and b (Figure 2) are the most likely candidates on the basis of RP-HPLC analysis of the deprotection reactions studied. Conversely, deprotection mechanisms according to paths c and d cannot, at this point, be conclusively confirmed or rejected.

To demonstrate the utility of **Rp-1** and **Sp-1**, the stereocontrolled synthesis of [**Rp**, **Rp**]- and [**Sp**, **Sp**]-trideoxycytidyl diphosphorothioate **d(C_{PS}C_{PS}C)**, and [**Rp**, **Sp**, **Rp**]-tetraoxycytidyl triphosphorothioate **d(C_{PS}C_{PS}C_{PS}C)** was attempted using a modified solid-phase protocol (see Experimental Section). Thus, the *P*-stereodefined 5'-*O*-DMTr-deoxyribonucleotide analogues were released from the solid support, *N*- and *P*-deprotected, and then purified by RP-HPLC. Following removal of the 5'-*O*-DMTr group from each purified oligonucleotides by treatment with 80% acetic acid, RP-HPLC chromatograms

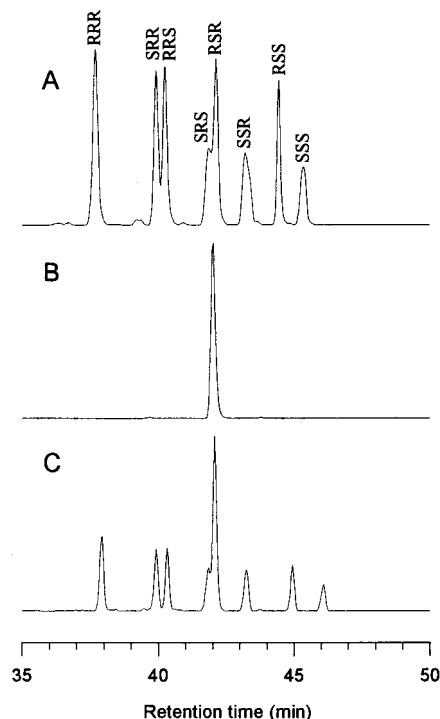


Figure 3. Panel A: RP-HPLC chromatogram of purified *P*-diastereomeric **d(C_{PS}C_{PS}C_{PS}C)** synthesized from standard solid-phase phosphoramidite chemistry using 3*H*-1,2-benzodithiol-3-one 1,1-dioxide as a sulfur-transfer reagent. Panel B: RP-HPLC chromatogram of purified [**R_p**,**S_p**,**R_p**]-**d(C_{PS}C_{PS}C_{PS}C)** synthesized from deoxyribonucleoside cyclic *N*-acylphosphoramidites **R_p-1** and **S_p-1** according to solid-phase techniques and by the use of 3*H*-1,2-benzodithiol-3-one 1,1-dioxide as a sulfur-transfer reagent. Panel C: RP-HPLC chromatogram of purified *P*-diastereomeric **d(C_{PS}C_{PS}C_{PS}C)** spiked with purified [**R_p**,**S_p**,**R_p**]-**d(C_{PS}C_{PS}C_{PS}C)**.

of [**R_p**, **R_p**]- and [**S_p**, **S_p**]-**d(C_{PS}C_{PS}C)**,¹³ and [**R_p**, **S_p**, **R_p**]-**d(C_{PS}C_{PS}C_{PS}C)** showed a single peak for each oligonucleotide analogue (Figure 3, panel B). For comparison, solid-phase syntheses of *P*-diastereomeric **d(C_{PS}C_{PS}C)** and **d(C_{PS}C_{PS}C_{PS}C)** were also performed using standard 2-cyanoethyl deoxyribonucleoside phosphoramidites and 3*H*-1,2-benzodithiol-3-one 1,1-dioxide²⁵ as the sulfur-transfer reagent. These oligomers were then deprotected and purified under conditions identical to those described above for the related *P*-stereodefined oligonucleotides. RP-HPLC analysis of *P*-diastereomeric **d(C_{PS}C_{PS}C)**¹³ and **d(C_{PS}C_{PS}C_{PS}C)** exhibited four and eight peaks, respectively, each peak corresponding to a specific *P*-diastereomer (Figure 3, panel A). The conspicuous absence of peaks corresponding to any of the seven diastereomers and the sole appearance of [**R_p**, **S_p**, **R_p**]-**d(C_{PS}C_{PS}C_{PS}C)** in Figure 3 (panel B) thus demonstrates that the new synthesis of the PS-ODN was achieved with complete *P*-stereospecificity.

The coupling efficiency of pyrimidine deoxyribonucleoside cyclic *N*-acylphosphoramidites was investigated further by attempting the solid-phase synthesis of [**R_p**]₁₁-**d[(T_{PS})₁₁T]** from **Sp-14** under the conditions used for *P*-stereodefined **d(C_{PS}C_{PS}C_{PS}C)**. The crude 5'-*O*-DMTr-dodecamer analogue was cleaved from the solid support, *P*-deprotected, and then analyzed by RP-HPLC.¹³ Following removal of the 5'-*O*-DMTr group, the crude oligodeoxyribonucleoside phosphorothioate was then subjected to polyacrylamide gel electrophoresis (PAGE) under denaturing conditions.¹³ Both RP-HPLC and PAGE show the dodecanucleotide as a major product. In the PAGE analysis, the band corresponding to the 12-mer accounts for ~75% of the combined intensity of all bands. These results indicate that

(30) (a) Wilk, A.; Srinivasachar, K.; Beaucage, S. L. *J. Org. Chem.* **1997**, *62*, 6712–6713. (b) Wilk, A.; Grajkowski, A.; Srinivasachar, K.; Beaucage, S. L. *Antisense Nucleic Acid Drug Dev.* **1999**, *9*, 361–366.

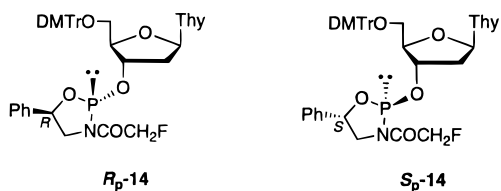
(31) (a) van Boom, J. H.; Burgers, P. M. J.; van Deursen, P. H.; Arentzen, R.; Reese, C. B. *Tetrahedron Lett.* **1974**, 3785–3788. (b) Adamiak, R. W.; Arentzen, R.; Reese, C. B. *Tetrahedron Lett.* **1977**, 1431–1434. (c) Reese, C. B.; Titmas, R. C.; Yau, L. *Tetrahedron Lett.* **1978**, 2727–2730.

(32) (a) Daub, G. W.; van Tamelen, E. E. *J. Am. Chem. Soc.* **1977**, *99*, 3526–3528. (b) Brill, W. K.-D.; Nielsen, J.; Caruthers, M. H. *J. Am. Chem. Soc.* **1991**, *113*, 3972–3980. (c) Caruthers, M. H.; Kierzek, R.; Tang, J. Y. In *Biophosphates and Their Analogues - Synthesis, Structure, Metabolism and Activity*; Bruzik, K. S., Stec, W. J., Eds; Elsevier: Amsterdam, 1987; pp 3–21.

(33) Ho, T.-L. *Chem. Rev.* **1975**, *75*, 1–20.

(34) Wilk, A.; Uznanski, B.; Stec, W. J. *Nucleic Acids Res. Symp. Ser. No. 24* **1991**, 63–66.

both thymidine and 2'-deoxycytidine cyclic *N*-acylphosphoramidites can confidently be used in the solid-phase synthesis of much larger oligomers.



In summary, the preparation of pyrimidine deoxyribonucleoside cyclic *N*-acylphosphoramidites is easily accomplished from commercially available precursors. Chromatographic resolution of these diastereomeric phosphoramidites to *P*-stereopure cyclic *N*-acylphosphoramidites such as **Rp-1** and **Sp-1** on silica gel is greatly facilitated by the difference in mobility of each diastereomer and that of its epimer. Base-assisted condensation of the 5'-OH function of a nucleoside or a nucleotide covalently linked to a solid support with **Rp-1** or **Sp-1** leads to rapid and efficient formation of an internucleoside phosphite triester linkage. The phosphite triester function can be either oxidized to a phosphate triester (PO) by treatment with *tert*-butyl hydroperoxide³⁵ or sulfurized by a sulfur-transfer reagent to a *P*-stereodefined thiophosphate phosphotriester (PS). This approach permits completely stereocontrolled synthesis of chimeric PO/PS-ODNs. In stark contrast, deoxyribonucleoside 3'-*O*-(2-thio-1,3,2-oxathiaphospholane) derivatives allow only the formation of polar *P*-stereodefined phosphorothioate diesters;⁵ an additional set of four deoxyribonucleoside 3'-*O*-(2-oxo-*spiro*-4,4-pentamethylene-1,3,2-oxathiaphospholane) monomers is required for the stereocontrolled synthesis of chimeric PO/PS-ODNs.^{5c,d}

The cyclic *N*-acylphosphoramidite approach to oligonucleotide synthesis is an attractive and versatile new concept in the preparation of *P*-stereopure oligonucleoside phosphorothioates. The method is currently being optimized to improve the chromatographic recovery of deoxyribonucleoside cyclic *N*-acylphosphoramidite monomers that will be used for incorporating the four standard nucleobases into DNA chains of at least 20 bases long. These oligonucleotides will include *P*-stereodefined and *P*-diastereomeric PS-ODNs, chimeric PO/PS-ODNs, and unmodified oligomers. Results of these studies will be reported in due course.

Experimental Section

Materials and Methods. Common chemicals and solvents were purchased from various commercial sources and used without further purification. Anhydrous pyridine and benzene were obtained from Aldrich and used as received. Acetonitrile (Aldrich) and *N,N,N',N'*-tetramethylguanidine (Aldrich) were refluxed over calcium hydride, and distilled prior to use. Phosphorus trichloride (Aldrich) was distilled immediately prior to use. (±)-2-Amino-1-phenylethanol, (*R*)-2-amino-1-phenylethanol, and (*S*)-2-amino-1-phenylethanol were purchased from Fluka and used as received. Ethyl fluoroacetate, *N*-(hydroxyethyl)-2,2,2-trifluoroacetamide, hexaethylphosphorus triamide, and sublimed 1*H*-tetrazole were purchased from Aldrich and used without further purification. Protected nucleosides such as *N*^t-benzoyl-5'-*O*-(4,4'-

dimethoxytrityl)-2'-deoxycytidine (Chem-Impex), *N*²-isobutyryl-5'-*O*-(4,4'-dimethoxytrityl)-2'-deoxyguanosine (Chem-Impex), and 3'-*O*-acetyl thymidine (Sigma) were used without additional purification. DNA synthesis reagents were purchased from PE-Biosystems and used according to the manufacturer's recommendations. The sulfur transfer reagent 3*H*-1,2-benzodithiol-3-one 1,1-dioxide was obtained from Glen Research and used as recommended in the literature.^{25b,c}

Flash chromatography on silica gel columns was performed using Merck silica gel 60 (230–400 mesh), whereas analytical thin-layer chromatography (TLC) was conducted on 2.5 cm × 7.5 cm glass plates coated with a 0.25 mm thick layer of silica gel 60 F₂₅₄ (Whatman) or on HPTLC–RP2F reversed phase 10 cm × 10 cm glass plates coated with a 0.15 mm thick layer of ethyl modified silica gel W/UV254 (Analtech). Analytical HPLC chromatography was achieved using a 4.6 mm × 250 mm Kromasil (Si-100, 5 μm) column (Supelco).

NMR spectra were recorded at 25 °C or as indicated at 7.05 T (300 MHz for ¹H). ¹H- and proton-decoupled ³¹P NMR spectra were obtained using deuterated solvents. Unless noted otherwise, tetramethylsilane (TMS) was used as internal reference for ¹H NMR spectra, and 85% phosphoric acid in deuterium oxide as an external reference for ³¹P NMR spectra. Proton-decoupled ¹³C NMR spectra were recorded in either CDCl₃, C₆D₆, or DMSO-*d*₆ using TMS as an internal reference. Proton-coupled ¹⁹F NMR spectra were recorded using fluorotrichloromethane as an external reference. Chemical shifts δ are reported in parts per million (ppm).

Nominal resolution and accurate mass electron-ionization (70 eV) mass spectra were acquired from samples introduced directly into the ion source via a solid's direct exposure (high temperature) probe using perfluorokerosene (PFK) as an internal standard. Nominal and accurate mass fast ion (cesium) bombardment mass spectra were acquired from samples dissolved in glycerol (to which aqueous sodium iodide was added) and bombarded with 8 keV fast cesium ions using cesium iodide or a mixture of cesium iodide and sodium iodide as a mass calibration standard.

(±)-2-[*N*-(2-Fluoroacetyl)amino-1-phenylethanol (**4**)]. Commercial (±)-2-amino-1-phenylethanol (**2**) (5.48 g, 40.0 mmol) and ethyl fluoroacetate (**3**) (5.30 g, 50.0 mmol) were heated at 130 °C until the generated ethanol had completely distilled off (~2 h). Upon cooling to ambient temperature, the reaction mixture solidified under high vacuum. The crude product was recrystallized from CHCl₃ to afford **4** (5.70 g, 28.9 mmol, 72%) as white crystals (mp 121–123 °C). ¹H NMR (300 MHz, DMSO-*d*₆) δ 3.21 (ddd, *J* = 13.4, 7.9, 5.5 Hz, 1H), 3.37 (m, 1H), 4.68 (m, 1H), 4.78 (d, *J* = 47.1 Hz, 2H), 5.49 (d, *J* = 4.3 Hz, 1H), 7.30 (m, 5H), 8.06 (t, *J* = 5.5 Hz, 1H). ¹³C NMR (75 MHz, DMSO-*d*₆) δ 54.2, 78.9, 87.9 (d, ¹*J*_{CF} = 180 Hz), 133.8, 135.0, 135.9, 151.3, 175.0 (d, ²*J*_{CF} = 17.0 Hz). EI–HRMS: calcd for C₁₀H₁₂FNO₂ (M⁺) 197.0852, found 197.0862.

2-(*N,N*-Diethylamino)-3-(2-fluoroacetyl)-5-phenyl-1,3,2-oxazaphospholane (**5**). Recrystallized **4** (4.93 g, 25.0 mmol) and hexaethylphosphorus triamide (6.20 g, 25.0 mmol) were heated at 120 °C until ~3.2 g of *N,N*-diethylamine was collected by distillation (~3 h). The reaction mixture was then distilled under high vacuum to give 5.79 g of **5** (19.2 mmol, 76%) as a slightly yellow viscous liquid (bp 150 °C at 0.3 mmHg). ³¹P NMR (121 MHz, C₆D₆) δ 119.0 (d, *J*_{PF} = 70.5 Hz), 123.6, 128.7 (d, *J*_{PF} = 52.9 Hz), 133.1. ³¹P NMR (121 MHz, DMSO-*d*₆) δ 115.6 (d, *J*_{PF} = 57.6 Hz), 122.3, 125.4 (d, *J*_{PF} = 74.7 Hz), 130.8. ¹⁹F NMR (282 MHz, C₆D₆) δ -229.9 (t, ²*J*_{FH} = 46.6 Hz), -229.3 (t, ²*J*_{FH} = 46.6 Hz), -225.4 (dt, *J*_{FP} = 70.3 Hz, ²*J*_{FH} = 47.4 Hz), -224.9 (dt, *J*_{FP} = 53.0 Hz, ²*J*_{FH} = 47.4 Hz). EI–HRMS: calcd for C₁₄H₂₀FN₂O₂ P (M⁺) 298.1247 found 298.1243.

2-[*N*-(2,2,2-Trifluoroacetyl)amino]ethyl phosphordichloridite (**6**). *N*-(2-Hydroxyethyl)-2,2,2-trifluoroacetamide (23.57 g, 0.15 mol) and anhydrous acetonitrile (35 mL) were placed in a flame-dried addition funnel. The solution was added, dropwise over a period of 2 h, to a 500 mL flame-dried round-bottom flask containing a stirred solution of freshly distilled phosphorus trichloride (24.76 g, 0.18 mol) in anhydrous acetonitrile (180 mL). During the course of the addition, a slight vacuum was applied through the dropping funnel to keep an internal pressure of ~750 mmHg, enabling removal of gaseous hydrogen chloride that was generated. The reaction mixture was then stirred for an additional 3 h at ~40 mmHg. The remaining material

(35) ³¹P NMR analysis of the aqueous iodine oxidation of **Rp-9** or **Sp-9** revealed a considerable loss of the benzylic phosphate protecting group during the course of the reaction. Our findings are in agreement with those reported by others (see ref 32c) on the sensitivity of internucleosidic *o*-methylbenzyl phosphite triesters to aqueous iodine. However, no premature loss of the benzylic phosphate-protecting group was observed when *tert*-butylhydroperoxide, instead of aqueous iodine, was used for the oxidation of **Rp-9** or **Sp-9**.

was distilled under reduced pressure to give the colorless phosphorodichloridite **6** (34.83 g, 0.13 mol, 87%). Bp: 91–94 °C/0.2 mmHg. ¹H NMR (300 MHz, C₆D₆) δ 2.85 (m, 2H), 3.62 (m, 2H). ¹³C NMR (75 MHz, C₆D₆) δ 39.3 (d, ¹J_{CP} = 3.9 Hz), 65.5 (d, ²J_{CP} = 9.7 Hz), 116.2 (q, ¹J_{CF} = 288 Hz), 157.3 (q, ²J_{CF} = 36.7 Hz). ³¹P NMR (121 MHz, C₆D₆) δ 178.1. EI–HRMS: calcd for C₄H₅Cl₂F₃NO₂P (M⁺ – HCl) 220.9621, found 220.9634. Upon prolonged standing (2 y) at –20 °C, phosphorodichloridite **6** cyclized to the chloro phosphine **7** (~60%) which was isolated by distillation as a mixture of rotamers **7a** and **7b**. Bp: 33–35 °C/0.2 mmHg. ¹H NMR (300 MHz, C₆D₆) δ 2.85 (m, 1H), 3.06 (m, 1H), 3.67 (m, 1H), 3.89 (m, 1H). ¹³C NMR (75 MHz, C₆D₆) δ 41.7, 43.0, 68.7 (d, ²J_{CP} = 7.7 Hz), 72.4, 116.0 (q, ¹J_{CF} = 288 Hz), 116.3 (q, ¹J_{CF} = 288 Hz), 157.2 (q, ¹J_{CF} = 36.7 Hz), 157.3 (q, ¹J_{CF} = 36.7 Hz). ³¹P NMR (121 MHz, C₆D₆) δ 145.9 (q, ¹J_{PF} = 74.2 Hz), 151.4. ¹⁹F NMR (282 MHz, C₆D₆) δ –74.4, –71.9 (d, ¹J_{FP} = 75.0 Hz). EI–HRMS: calcd for C₄H₄ClF₃NO₂P (M⁺) 220.9621, found 220.9622.

N⁴-Benzoyl-5'-O-(4,4'-dimethoxytrityl)-3'-O-[3-(2-fluoroacetyl)-5-phenyl-1,3,2-oxazaphospholanyl]-2'-deoxycytidine (R_P-1 and S_P-1). To a solution of vacuum-dried **8** (1.90 g, 3.0 mmol) and phosphinylating reagent **5** (980 mg, 3.3 mmol) in dry acetonitrile (15 mL) was added via syringe a 0.4 M solution of 1*H*-tetrazole in dry acetonitrile (8.3 mL, 3.3 mmol). The reaction mixture was stirred at room temperature (20 min) until only traces (~1–2%) of unreacted **8** could be detected by HPTLC analysis. The reaction mixture was then concentrated to a volume of ~4 mL under reduced pressure, and applied to the top of a silica gel (Merck 9385, 230–400 mesh, 60 Å, 45 g) chromatography column (3.5 cm ID × 10 cm) equilibrated in CHCl₃–CH₃CN (3:1). The column was eluted with a linear gradient of CHCl₃–CH₃CN (3:1 v/v) to CHCl₃–CH₃CN (25:10) to afford pure **S_P-1** (300 mg, 0.35 mmol) and **R_P-1** (232 mg, 0.27 mmol) as white amorphous solids. A mixture of **R_P-1** and **S_P-1** was also isolated (739 mg, 0.86 mmol).

An alternate route to the preparation of **R_P-1** and **S_P-1** relied on the addition of anhydrous acetonitrile (5 mL) to vacuum-dried **8** (1.00 g, 1.58 mmol) and 1*H*-tetrazole (111 mg, 1.58 mmol). To the stirred solution was added phosphoramidite **5** (520 mg, 1.75 mmol), dropwise by syringe, over 15 min. Thin-layer chromatography was used to monitor the reaction to completion. The reaction mixture was evaporated to a foam under reduced pressure. Ethyl acetate (3 mL) was added to the foamy residue, and the resulting suspension was applied to a short silica gel (Merck 9385, 230–400 mesh, 60 Å, 67 g) chromatography column (9.0 cm ID × 2 cm) equilibrated in EtOAc. The flask containing crude **R_P-1** and **S_P-1** was rinsed with fresh EtOAc (2 mL), which was added to the top of the column after the first EtOAc layer had dispersed through the column. Further elution with EtOAc gave **S_P-1** (302 mg, 0.35 mmol) and **R_P-1** (359 mg, 0.42 mmol) as white foamy solids. As above, a mixture of **R_P-1** and **S_P-1** was also isolated (198 mg, 0.23 mmol). HPTLC–RP2F (Analtech): **R_P-1**, *R_f* (CHCl₃:CH₃CN 2:1 v/v) = 0.51; **S_P-1**, *R_f* (CHCl₃:CH₃CN 2:1 v/v) = 0.71. Analytical HPLC analysis of **R_P-1** and **S_P-1** was performed on a Supelco Kromasil (Si-100, 5 μm) column (4.6 mm × 250 mm) using a linear gradient of EtOAc (1%/min) from 70% EtOAc in hexane at a flow rate of 2.0 mL/min. Under these conditions, the retention time *t_R* of **S_P-1** and **R_P-1** on the column is 8.4 and 17.4 min, respectively. ³¹P NMR (121 MHz, CD₃CN) **R_P-1** δ 131.1 (d, ¹J_{PF} = 135 Hz), 135.9; **S_P-1** δ (ppm) 128.8 (d, ¹J_{PF} = 128 Hz), 132.6. ³¹P NMR (121 MHz, C₆D₆): **R_P-1** δ 127.0 (d, ¹J_{PF} = 188 Hz), 134.0; **S_P-1** δ (ppm) 126.0 (d, ¹J_{PF} = 182 Hz), 133.0. ¹⁹F NMR (282 MHz, C₆D₆) **R_P-1** δ –218.3 (dt, ¹J_{FP} = 189 Hz, ²J_{FF} = 46.6 Hz), –227 (dt, ⁴J_{FP} = 3.8 Hz, ²J_{FF} = 46.6 Hz); **S_P-1** δ –218.5 (dt, ¹J_{FP} = 181 Hz, ²J_{FF} = 46.6 Hz), –224.2 (dt, ⁴J_{FP} = 2.1 Hz, ²J_{FF} = 46.6 Hz). FAB–HRMS: **R_P-1**: calcd for C₄₇H₄₄FN₄O₉P (M + Na⁺) 881.2728, found 881.2687; **S_P-1**: calcd for C₄₇H₄₄FN₄O₉P (M + Na⁺) 881.2728, found 881.2653.

5'-O-(4,4'-Dimethoxytrityl)-3'-O-[3-(2-fluoroacetyl)-5-phenyl-1,3,2-oxazaphospholanyl] thymidine (R_P-14 and S_P-14). The deoxyribose nucleoside cyclic *N*-acylphosphoramidites **R_P-14** and **S_P-14** were prepared under conditions identical to those used for the synthesis of **R_P-1** and **S_P-1** and were isolated in similar yields. ³¹P NMR (121 MHz, C₆D₆) **R_P-14** δ 131.1 (d, ¹J_{PF} = 135 Hz), 135.9; **S_P-14** δ (ppm) 128.9 (d, ¹J_{PF} = 131 Hz), 133.2. FAB–HRMS: **R_P-14**: calcd for C₄₁H₄₁FN₃O₉P

(M + Cs⁺) 902.1618, found 902.1644; **S_P-1**: calcd for C₄₁H₄₁FN₃O₉P (M + Cs⁺) 902.1618, found 902.1643.

General Procedure for Manual Solid-Phase Synthesis of [R_P, R_P]- and [S_P, S_P]-d(C_{PS}C_{PS}C), [R_P, S_P, R_P]-d(C_{PS}C_{PS}C_{PS}C), and [R_P]₁₁-d[(T_{PS})₁₁T]. [R_P, R_P]-C_{PS}C_{PS}C: A standard DMT-dC^{Bz}-LCAA-CPG column (0.2 μmol) was subjected to the following sequence of steps: 1, 2, 3, 2, 3, 4, 1, 2, 3, 2, 3, 5. Step 1: 3% TCA (w/v)/CH₂Cl₂ (3 mL, 1 min), followed by washing with dry MeCN (3 mL, 30 s). Step 2: **S_P-1**, (5 mg, ~5 μmol) and TMG (4 μL, ~30 μmol) in dry MeCN (200 μL), 5 min, followed by washing with MeCN (3 mL, 30 s). Step 3: 0.05 M 3*H*-1,2-benzodithiol-3-one 1,1-dioxide in MeCN (200 μL), 3 min, followed by washing with MeCN (3 mL, 30 s). Step 4: Ac₂O/2,6-lutidine/THF (1 mL), mixed with 1-methylimidazole/THF (1 mL), 2 min, followed by washing with MeCN (3 mL, 30 s). Step 5: Concentrated NH₄OH (1 mL, 10 h, 55 °C). [S_P, S_P]-C_{PS}C_{PS}C: identical to the preparation of [R_P, R_P]-C_{PS}C_{PS}C except that **R_P-1** was used in step 2. [R_P, S_P, R_P]-C_{PS}C_{PS}C_{PS}C: A standard DMT-dC^{Bz}-LCAA-CPG column (0.2 μmol) was subjected to the following sequence of steps: 1, 2, 3, 2, 3, 4, 1, 2', 3, 2', 3, 4, 1, 2, 3, 2, 3, 5. Steps were identical to those used for the preparation of [R_P, R_P]-C_{PS}C_{PS}C except that **R_P-1** was used in step 2' which otherwise was identical to step 2. [R_P]₁₁-d[(T_{PS})₁₁T]: A column filled with DMT-T covalently attached to LCAA-CPG (0.2 μmol) through a succinyl-sarcosyl linker³⁶ was subjected to the following sequence of steps: (1, 2, 3, 2, 3, 4)₁₀, 1, 2, 3, 2, 3, 5. Steps were identical to those used for the preparation of [R_P, R_P]-C_{PS}C_{PS}C except that **S_P-14** was used in step 2.

Each ammoniacal solution collected from step 5 was concentrated under reduced pressure, and the crude oligomer was purified “trityl on” by RP-HPLC using a 5 μm Supelcosil LC-18S column (25 cm × 4.6 mm) and a linear gradient of 1% MeCN/min, starting from 0.1 M triethylammonium acetate pH 7.0, at a flow rate of 1 mL/min. Appropriate fractions were pooled together, evaporated to dryness under vacuum, and treated with aqueous 80% AcOH for 30 min. After removal of excess acid under low pressure, the purified oligonucleotide was dissolved in distilled water and further analyzed by RP-HPLC using the same column and chromatographic conditions as those employed for the purification of the crude oligonucleotide. RP-HPLC chromatogram of [R_P, S_P, R_P]-C_{PS}C_{PS}C_{PS}C is shown in Figure 3, whereas chromatograms of [R_P, R_P]-C_{PS}C_{PS}C and [S_P, S_P]-C_{PS}C_{PS}C are displayed as Supporting Information. In the case of unpurified [R_P]₁₁-d[(T_{PS})₁₁T], the “trityl on” RP-HPLC chromatogram and a photograph of its “trityl off” PAGE profile are shown as Supporting Information.

Acknowledgment. This research was supported in part by an appointment to the Postgraduate Research Participation Program at the Center for Biologics Evaluation and Research administered by the Oak Ridge Institute for Science and Education through an interagency agreement between the U.S. Department of Energy and the U.S. Food and Drug Administration.

Supporting Information Available: ¹H and ¹³C NMR spectra of **4** and **5**. ³¹P NMR spectra of **R_P-1**, **S_P-1**, **5**, **6**, **7**, **R_P-9**, **S_P-9**, **R_P-10**, **R_P-11**, **S_P-11**, **S_P-12**, and **S_P-14**. ¹⁹F NMR spectra of **S_P-1**, **5**, and **7**. RP-HPLC Chromatograms of **R_P-13** and **S_P-13**, [R_P, R_P]- and [S_P, S_P]-d(C_{PS}C_{PS}C), *P*-diastereomeric d(C_{PS}C_{PS}C), “trityl on” [R_P]₁₁-d[(T_{PS})₁₁T], and PAGE profile of “trityl off” [R_P]₁₁-d[(T_{PS})₁₁T] (PDF). This material is available free of charge via the Internet at <http://pubs.acs.org>.

JA991773U

(36) This CPG support was prepared as reported in the literature; see: Brown, T.; Pritchard, C. E.; Turner, G.; Salisbury, S. A. *J. Chem. Soc., Chem. Commun.* **1989**, 891–893.

(37) Boal, J. H.; Wilk, A.; Harindranath, N.; Max, E. E.; Kempe, T.; Beaucage, S. L. *Nucleic Acids Res.* **1996**, *24*, 3115–3117.